

A novel photographic approach for monitoring the structural heterogeneity and diversity of grassland ecosystems

Raphaël Proulx^{1,*}, Irene T. Roca¹, Felipe S. Cuadra²,
Ian Seiferling¹ and Christian Wirth²

¹ Chaire UQTR en Biologie Systémique de la Conservation, Université du Québec à Trois-Rivières, 3351 Des Forges, Trois-Rivières, Quebec G9A 5H7, Canada

² Department of Special Botany and Functional Biodiversity Research, Institute of Biology I, University of Leipzig, Johannisallee 21-23, 04103 Leipzig, Germany

*Correspondence address. Chaire UQTR en Biologie Systémique de la Conservation, Université du Québec à Trois-Rivières, 3351 Des Forges, Trois-Rivières, Quebec G9A 5H7, Canada. Tel: +1-819-376-5011; Fax: +1-819-376-5084; E-mail: raphael.proulx@uqtr.ca

Abstract

Aims

Studies that investigate the space-filling heterogeneity of biological structures in plant communities remain scarce. The main objective of this study was to evaluate the relationship between newly developed photographic measures of structural heterogeneity in digital images and plant species composition in the context of a long-term grassland experiment.

Methods

We tested a close-range photographic protocol using measures of structural heterogeneity in gray-tone images, namely mean information gain (MIG) and spatial anisotropy, to assess differences in the compositional (species richness) and functional characteristics (plant height and flowering) of 78 managed grassland communities. We also implemented a random placement model of community assembly to explore the links between our measures of structural complexity and the geometric pattern of plant communities.

Important Findings

MIG and spatial anisotropy correlated with the growth and species richness of grassland communities. Simulations showed that structural heterogeneity in gray-tone digital images is a function of the size distribution and orientation pattern of plant modules. This easy, fast and non-destructive methodological approach could eventually serve to monitor the diversity and integrity of various ecosystems at different resolutions across space and time.

Keywords: biodiversity, photography, ecosystem integrity, texture, random placement model

Received: 7 August 2013, Revised: 25 November 2013,
Accepted: 7 December 2013

INTRODUCTION

Among the foundations of ecology, we find the concept that ecosystems develop toward a state of increasing biomass (Christensen 1995; Margalef 1963; Odum 1969) and heterogeneity of biological structures (e.g. Carroll 2001; von Bertalanffy 1950). The link between standing biomass and structural heterogeneity in plant communities was first formalized by Weller's interspecific size–density relationship and summarized in the following terms (Weller 1989): ‘Biomass is maximal when the available growing surface is fully used,

the stand is as tall as possible, and the stand packs the maximum possible amount of biomass into each cubic meter of space occupied’. In this context, structural heterogeneity is the geometric pattern made by aboveground plant modules (e.g. stems, leaves, twigs and flowers) within a given volume space. Crowded plant communities consisting of many canopy individuals over a dense understory should be structurally more heterogeneous than unfilled communities with just a few tall individuals and a sparse understory. While Weller's (1989) model could be used to assess the structural heterogeneity of vegetation stands, the study of the relationship

between biomass and plant density is time consuming and destructive.

Proulx and Parrott (2008) recently proposed quantifying the structural heterogeneity of forest communities using an information theoretic measure of texture in gray-tone digital images. Their close-range photographic approach captures, in two dimensions (the image space), the three-dimensional geometric structure of plant communities. Preliminary results indicated that (i) the maximum of structural heterogeneity in digital images was attained at the seasonal peak of tree foliage development and (ii) image structural heterogeneity correlated positively with species richness of the understory vegetation (Proulx and Parrott 2008). Subsequent studies have also found positive correlations between similar image-derived texture metrics and biodiversity measures in bird (Bellis *et al.* 2008; St-Louis *et al.* 2009), forest (Getzin *et al.* 2011) and coral reef fish communities (Mellin *et al.* 2012).

From a geometrical standpoint, plant communities should increase in structural heterogeneity when individuals maximize their use of resources while subject to both physical and biological constraints like gravity, solar radiation, herbivory and competition for water and nutrients (Marks and Lechowicz 2008; Niklas 1994; Reu *et al.* 2011). Packing too much phytomass per unit of volume may compromise vital processes such as reproduction and growth, whereas too little phytomass may indicate a sub-optimal use of otherwise available resources. For example, species-poor communities comprising plants with similar heights, or flowering patterns, may show more regular structures than species-rich communities consisting of plants with a broader range of statures and inflorescence types. However, we do not know whether such compositional differences can be captured using photographic indices of structural heterogeneity in grassland communities.

The principal objective of this study is to investigate the relationship between non-destructive measures of structural heterogeneity in gray-tone digital images and plant species composition within the setting of a long-term grassland experiment (cf. Roscher *et al.* 2004). The Jena Experiment (Thuringia, Germany, 50°55'N, 11°35'E, 130 m.a.s.l.) was specifically designed to study the effect of plant species richness on the functioning of managed grassland ecosystems, independent of species composition and abiotic environmental factors. Using the design of the Jena Experiment, we asked two research questions: Question I (Q1): does the structural heterogeneity of grassland communities covary with plant species richness and development time? To address this question, we used a novel photographic method for assessing the structural heterogeneity of plant communities using close-range digital imagery. Question II (Q2): can the structural heterogeneity of the vegetation be explained by functional descriptors of grassland communities? To address this question, we developed two models: first, a dead-leaves geometric model of community assembly and, second, a statistical framework relating our measure of structural heterogeneity

in gray-tone images against rapidly assessed, visual descriptors of grassland communities.

MATERIALS AND METHODS

Experimental set-up

The Jena Experiment was established in May 2002 on former agricultural fields within the floodplain of the river Saale near Jena (Thuringia, Germany, 50°55'N, 11°35'E, 130 m.a.s.l.). The main experiment comprises 78 plots of 400 m² with five levels of plant species richness (1, 2, 4, 8 and 16 species), for which 16 replicates exist for each 1-, 2-, 4- and 8-species level, while 14 replicates exist for the 16-species level. Species used in monocultures and mixtures were selected randomly from a pool of 60 species common to the Central European grasslands. The site is regularly weeded to maintain the species composition of experimental communities and is harvested twice a year (early June and late August).

Between 28 April 2010 (1 week after weeding) and 01 June 2010 (1 week before the first biomass harvesting), we repeatedly surveyed all grassland communities. Here, we delineated a smaller, 2 × 2 m sub-plot inside each of the larger plots. Starting at the northeastern corner of the sub-plot and moving in a clockwise direction, we marked 1-cm increments with a measuring tape along the sub-plot perimeter and delineated four intervals: 1–200 cm (east side of sub-plot), 201–400 cm (south side), 401–600 cm (west side) and 601–800 cm (north side). During each survey, we identified 12 individuals (i.e. single tillers, shoots or rosettes) by randomly selecting three positions within each of the four sub-plot intervals. At each randomly selected position along the sub-plot perimeter, we identified the closest individual plant located 30 cm inside the sub-plot margin.

We completed a vegetation survey of all 78 experimental grassland communities for three separate growth periods prior to the first harvest: May 04 (April 28–May 04), May 18 (May 12–May 18) and June 01 (May 26–June 01). During each visit, and for each randomly identified individual plant, we recorded the species name, the presence/absence of a visible inflorescence and the vegetative height (following Cornelissen *et al.* 2003). From each visit to the experimental plots, we calculated flowering intensity as the percentage of individuals bearing flowers and mean plant height as the arithmetic mean of individuals' height.

Photographic set-up

Using a point-and-shoot digital camera (PowerShot A480, Canon Inc., Tokyo, Japan), we captured close-range digital images of the grassland communities on the three different occasions corresponding to our growth periods (i.e. May 04, May 18 and June 01). We photographed each 2 × 2 m sub-plot (grassland community) from a side view perspective (i.e. the camera 1 m above the ground, tilted at 45° down the horizontal plane and the lens pointed at the sub-plot center) at a distance of 0.1 m outside the sub-plot's perimeter (Fig. 1).

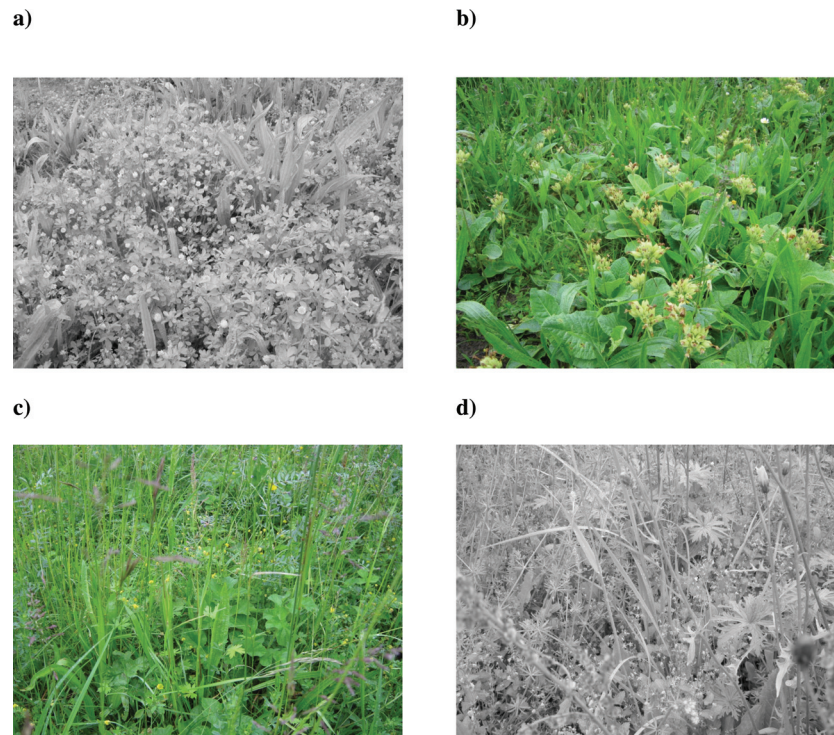


Figure 1: selection of close-range digital images used to assess the structural heterogeneity of grassland communities in the Jena Experiment. The panels show different image patterns for the (a) 2-species, (b) 4-species, (c) 8-species and (d) 16-species grassland communities.

We shot all images under an overcast sky between 11h00 and 13h00 and relied on the camera's internal light meter to adjust the image exposure to a reference value, i.e. adjusting the camera's lens aperture diameter and shutter speed based on luminance conditions. The focus distance was determined using the multi-zone metering system of the camera while all other camera parameters were kept constant at a focal length of 35 mm, ISO 100, automatic white balance and f-number f/3. Our decision to use a low-cost commercial camera was motivated by our intent to keep the photographic procedure as simple and accessible as possible.

During each of the three growth periods, we captured four images (one from each lineal side) of each grassland community. Out of this set of four images, we retained only the one with the highest texture value for subsequent analyses (see section Q1). Since factors like wind, depth shading and out-of-focus objects tend to smooth the image and, hence, arbitrarily decrease image texture values, we conducted this screening procedure to remove their potential effects. We recorded all images in a low-compression JPEG format of 2272×1704 pixels. We did not apply other post-processing routines to our images.

The photographic set-up was premised on the principle that close-range digital images taken from a side-view perspective capture both the horizontal and the vertical heterogeneity of biological structures in plant communities. Shooting images with a side-view 45° angle allowed us to capture, in two dimensions (the image space), the geometric structure

of plant communities that is represented in three dimensions (the volume space).

Q1: Mean information gain in gray-tone digital images as a measure of structural heterogeneity

The structural heterogeneity metric proposed by Proulx and Parrott (2008, 2009) is an information theoretic measure of texture called MIG (mean information gain). To calculate the MIG metric, we first transformed our Red-Green-Blue (RGB) 8-bits digital images into gray-tone images by computing the digital number average of the three channels: gray tones = $(R + G + B)/3$. MIG then determines the amount of spatial randomness in the pattern of gray-tone pixels as follows:

$$\text{MIG} = \frac{\left[-\sum_{i=1}^{M^k} p(\chi_i) \log p(\chi_i) \right] - \left[-\sum_{i=1}^M p(\gamma_i) \log p(\gamma_i) \right]}{\log(M^k/M)} = \frac{\text{JE} - \text{ME}}{\log(M^k/M)},$$

where $p(\gamma_i)$ is the probability of observing a pixel of value γ_i across M possible discrete gray-tone categories and $p(\chi_i)$ expresses the probability of finding a gray-tone spatial configuration χ_i of k -neighboring pixels forming a square of 2×2 pixels. M^k thus represents the maximum number of possible spatial configurations χ_i . Specifically, a co-occurrence matrix is tabulated by associating each pixel's gray-tone value (i, j) with the gray-tone values of adjacent pixels immediately below ($i+1, j$), in diagonal ($i+1, j+1$) and to the right ($i,$

$j+1$). Expressions within brackets in Equation (1) represent the joint Shannon entropy (JE) and the marginal Shannon entropy (ME) calculated from the co-occurrence matrix of gray-tone pixel values (Proulx and Fahrig 2010; Proulx and Parrott 2009). The fixed quantity $\log(M^k/M)$ normalizes MIG over the range 0–1. MIG is nearly zero ($MIG \rightarrow 0$) for uniform structural patterns and is maximal ($MIG \rightarrow 1$) for random ones. For our purposes here, we used a parameterization of $M = 15$ and $k = 4$.

We also determined if the geometric pattern of plant structures was more heterogeneous along one preferential image direction. We thus calculated a measure of anisotropy in the image as the ratio of MIG values (Equation (1)) obtained along the horizontal and vertical directions as follows: anisotropy = $MIG_{\text{horizontal}}/MIG_{\text{vertical}}$. To do so, we assembled a co-occurrence matrix considering only pairs of neighbor pixels oriented along either the horizontal (i.e. each pixel (i, j) and its adjacent right neighbor $(i, j+1)$ in the image) or the vertical image direction (i.e. each pixel (i, j) and its adjacent bottom neighbor $(i+1, j)$ in the image). Anisotropy characterizes the relative increase in the horizontal heterogeneity of plant structures in grassland images and takes values above one (anisotropy > 1) when MIG is comparatively higher along the horizontal than vertical direction.

Using the randomized species design of the Jena Experiment, we performed an analysis of covariance (ANCOVA) testing for the effect of the covariable plant species richness (quantitative variable fitted as a log-linear effect), the growth period (categorical variable with three levels: May 04, May 18 and June 01) and their interaction, on the two measures of structural heterogeneity (MIG and anisotropy) calculated from gray-tone images of grassland communities.

Q2—Model 1: A geometric model of the plant diversity–structural heterogeneity relationship

Lee et al. (2001) showed that the statistical properties of natural images can be captured by a dead-leaves geometric model. The fundamental basis of the model being that, natural images consist of a mosaic of opaque objects in a volume space which, in turn, occlude each other in the image space. Each model's run proceeds as follows: (i) generate an image of a prescribed size $S \times S$, (ii) randomly pick the size s of an object from a power function $f(s)$ of exponent α :

$$f(s) = s^{-\alpha}, \text{ where } s_{\text{min}} \leq s \leq s_{\text{max}},$$

(iii) choose a gray-tone intensity for this object, at random, from a uniform distribution, (iv) choose, at random, from a uniform distribution a pixel position on the image and place the object there and (v) repeat steps (ii)–(iv) iteratively until the image is completely covered by a set of objects partially occluding each other as in natural images. We herein implemented a dead-leaves model with the following parameters: $S = 2000$ pixels, $s_{\text{min}} = 10$ pixels and $s_{\text{max}} = 1800$ pixels, and fixed N to 15 gray-tone categories. We determined the parameters s_{min} and s_{max} by manually inspecting our

grassland community images to find the smallest and the largest object visible at the forefront of an image, i.e. objects not occluded by others, like flower, stem or leaf modules.

Lee et al. (2001) have shown that in the case of natural images, the α exponent of the power function $f(s)$ should be around three ($\alpha = 3$), referring to this parameterization as the 'law of cubic sizes'. However, the α exponent characterizing the size distribution of objects (i.e. plant modules) in close-range digital images may change over time because plant individuals in taller communities are closer to the camera lens. The direct consequence of depicting larger plant modules than expected by the law of cubic size would be to pull down the true α exponent below three ($\alpha < 3$). To illustrate this effect in our dead-leaves model simulations, we used several parameterizations of the power function ranging from $\alpha = 2.8$, approximating the law of cubic size, to $\alpha = 2.0$, reflecting the potential effect of vegetation growth on the size distribution of plant modules.

Lee et al. (2001) also proposed to use an ellipsoid as the primitive object shape in 'vegetation-like' simulations and, accordingly, we too applied this principle to the model. For each model iteration run, we bounded an ellipse's major axis of size s between s_{min} and s_{max} . We then randomly sampled the minor axis from a uniform distribution in the range $[s/4-s/2]$ (Lee et al. 2001). Typically, ellipsoid objects in a dead-leaves model are placed with their major axis either horizontally or vertically oriented with a 50/50 probability. Therefore, to simulate an anisotropic process here, we used different parameterizations of the horizontal/vertical orientation probability ranging between 0.52/0.48 and 0.38/0.64.

Finally, we calculated the MIG and anisotropy of dead-leaves modeled images and graphically compared the simulation results to the observed relationships obtained on the basis of the gray-tone images taken of the 78 experimental grassland communities. All simulations were performed using the `compute_dead_leaves_image` function distributed by Matlab Central (MathWorks, Natick, USA) under the BSD copyright license.

Q2—Model 2: A statistical model of the plant diversity–structural heterogeneity relationship

We explored if the structural heterogeneity of gray-tone images can be explained by two visual descriptors of plant communities. To this end, we fitted a mixed-effect regression model to structural heterogeneity metrics using mean plant height and flowering intensity as fixed effects while including the experimental plot as a random effect. Mean plant height defines the vertical dimension of the volume space in which the growth of aerial plant modules takes place. Thus, while mean plant height should increase the relative frequency of large-sized plant modules, both inter- and intra-specific competition for light resources per unit of volume should increase the frequency of small-sized plant modules in an image. The presence of flowers is another descriptor modifying the geometrical pattern of herbaceous communities that

can be detected in close-range digital images (e.g. Crimmins and Crimmins 2008; Thorp and Dierig 2011). We, therefore, regressed mean plant height and flowering intensity against MIG and anisotropy metrics in two separate statistical models. All statistical analyses were conducted using the R 3.0.1 software.

RESULTS

Q1: MIG as a measure of structural heterogeneity

MIG decreased with increasing plant species richness (Fig. 2). Results from the ANCOVA showed that the linear relationship between MIG and the logarithm of plant species richness was significantly different from zero [degrees of freedom (df) = 1; F = 78.43, P < 0.001]. Slopes did not differ among growth periods (df = 2; F = 3.042, P > 0.05), yet we did find a significant difference of intercepts among growth periods (df = 2; F = 100.33, P < 0.001; Fig. 2). Overall, the statistical model explained 54% of the variance in MIG values calculated from gray-tone images of grassland communities.

Anisotropy increased with increasing plant species richness, with values above one indicating more heterogeneity in the horizontal direction relative to the vertical (Fig. 3). The ANCOVA model revealed a significant linear relationship between the logarithm of plant species richness and anisotropy (df = 1; F = 59.34, P < 0.001), as well as a difference of intercepts among growth periods (df = 2; F = 16.74, P < 0.001) but no interaction (df = 2; F = 1.41, P > 0.05). The statistical model explained 27% of the variance in anisotropy values calculated from gray-tone images of grassland communities.

Q2: Models of the plant diversity–structural heterogeneity relationship

Simulations showed that MIG relates positively to the exponent α of the dead-leaves model (Fig. 2). MIG decreases linearly from around $MIG \approx 0.50$ when α is close to 3, to around $MIG \approx 0.35$ when α is approaching 2, suggesting that the structural heterogeneity of grassland images is contingent on the size distribution of plant modules (dashed black line; Fig. 2). As expected, dead-leaves model simulations showed

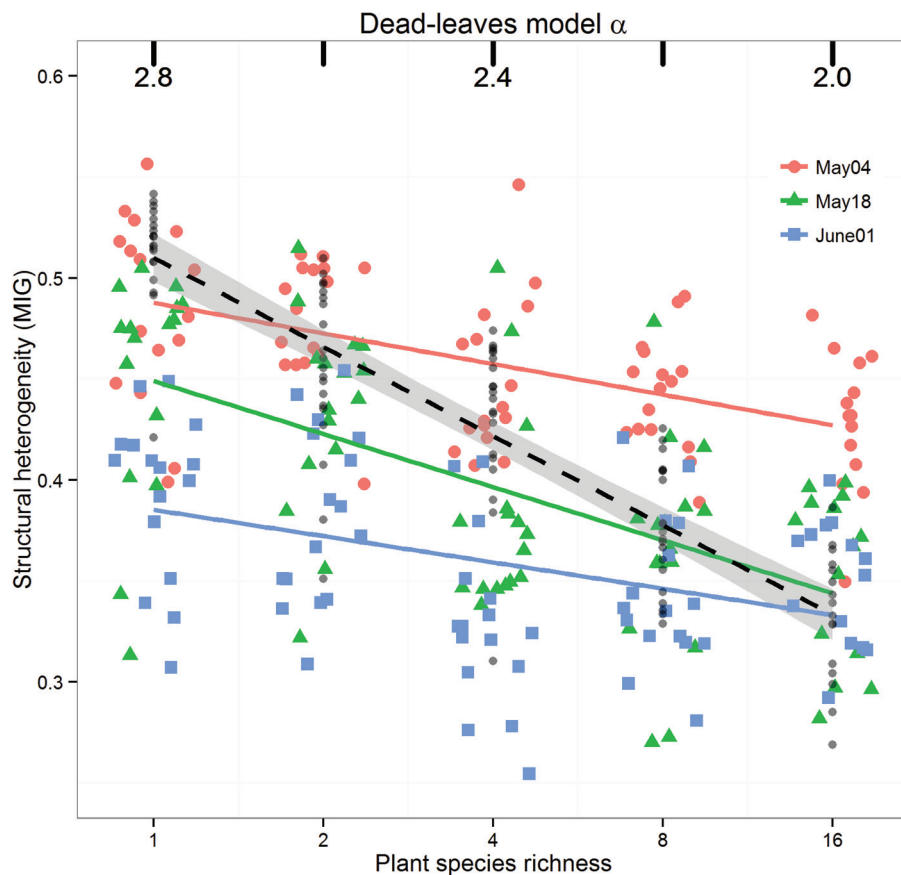


Figure 2: effect of plant species richness on MIG, a measure of structural heterogeneity calculated from the gray-tone images of 78 grassland communities photographed on three different occasions (May 04, May 18 and June 01). Plant species richness is expressed on a logarithmic scale. MIG values at each richness level appear slightly jittered. Are superimposed the results of a dead-leaves geometric model (dashed black line), in which the α exponent is a parameter characterizing the size distribution of objects (plant modules) in a gray-tone simulated image. A total of 20 gray-tone images were simulated at each of five α exponent values: 2.8, 2.6, 2.4, 2.2 and 2.0.

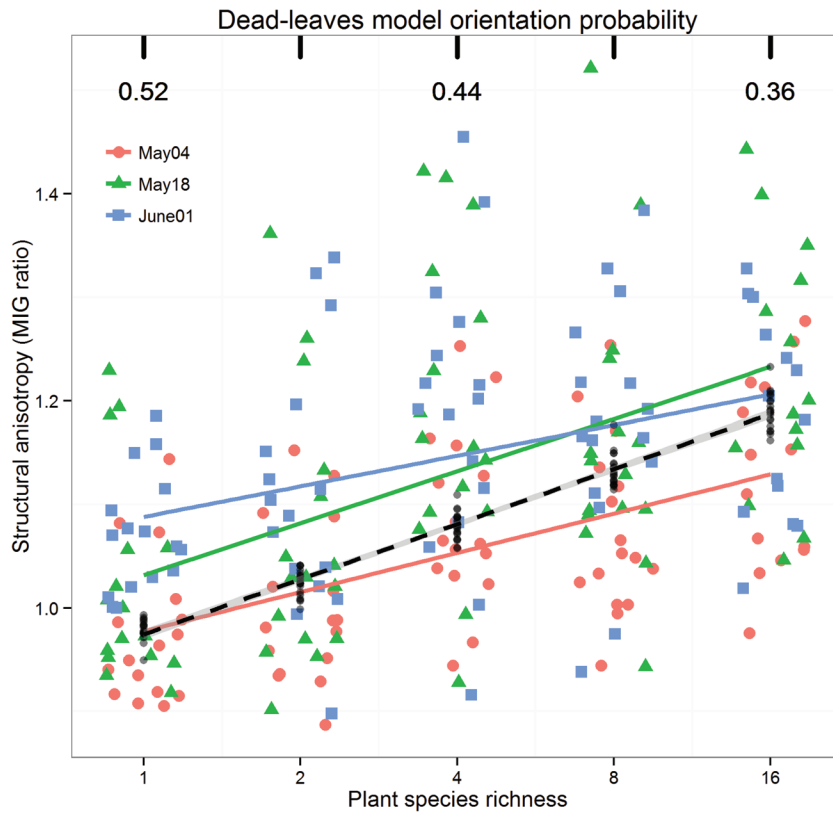


Figure 3: effect of plant species richness on anisotropy ($MIG_{horizontal}/MIG_{vertical}$), a measure of structural heterogeneity calculated from the gray-tone images of 78 grassland communities photographed on three different occasions (May 04, May 18 and June 01). Plant species richness is expressed on a logarithmic scale, while anisotropy values at each richness level appear slightly jittered. Are superimposed the results of a dead-leaves geometric model (dashed black line), in which the orientation probability is a parameter determining the probability that the major axis of an ellipsoid object in the image falls along the horizontal direction. A total of 20 gray-tone images were simulated at each of five orientation probability values: 0.52, 0.48, 0.44, 0.40 and 0.36.

that anisotropy is positive when the ellipsoid objects in an image are horizontally oriented with a relative probability under 0.5 (dashed black line; Fig. 3).

Mean plant height and flowering intensity community descriptors explained a significant amount of variation in MIG and anisotropy (Table 1). Mean plant height alone explained 38 and 27% of the total variation in MIG and anisotropy, respectively (Table 1). Flowering intensity was correlated positively to mean plant height (Pearson’s $r = 0.52$) and explained little of the residual variation in MIG and anisotropy.

DISCUSSION

In this study, we have shown that non-destructive measures of structural heterogeneity in gray-tone digital images correlated well with plant species richness and growth in managed grasslands. Our preliminary findings indicated that structural heterogeneity metrics, calculated from gray-tone images of grasslands, were best explained by mean plant height, which defines the vertical dimension of the community and increases the frequency of large-sized stems and leaves in the image.

Table 1: mixed-effect regression coefficients and statistics for mean plant height and flowering intensity descriptors in relation to measures of MIG and anisotropy ($MIG_{horizontal}/MIG_{vertical}$) of grassland’s gray-tone images ($n = 228$)

Fixed effect	Coefficient	t-Value	Univariate R^2
MIG			
Mean plant height	$-2.7e^{-3}$	-9.12	0.38
Flowering intensity	$-5.0e^{-4}$	-3.52	0.25
Anisotropy			
Mean plant height	$3.1e^{-3}$	5.74	0.27
Flowering intensity	$4.1e^{-4}$	1.40	0.14

The coefficients of determination (univariate R^2) were obtained by fitting a linear regression model to each variable independently.

MIG as a measure of structural heterogeneity

MIG and anisotropy metrics calculated from close-range natural images did capture structural heterogeneity differences in the geometrical pattern of plant communities. We found that MIG values decreased with increasing plant species richness, varying on average from around $MIG \approx 0.45$ in monocultures and 2-species communities to around

MIG \approx 0.35 in 8- and 16-species communities. Moreover, anisotropy values ($MIG_{\text{horizontal}}/MIG_{\text{vertical}}$) increased with increasing plant species richness, revealing more heterogeneous patterns in the horizontal than vertical image direction of species-rich communities. Furthermore, our results showed marked differences in, both, MIG and anisotropy metrics among growth periods, as MIG decreased, whereas anisotropy increased with increasing growth time of grassland communities.

In a previous study, Proulx and Parrott (2008) assessed the potential of MIG as a measure of plant structural heterogeneity in gray-tone digital images of forest stands. Consistent with the findings presented here, they reported patterns departing from higher MIG values early in the growing season, toward that of lower intermediate values when the leaf biomass was at its summer peak (MIG \approx 0.35; Proulx and Parrott 2008). The observed decrease in image heterogeneity with increasing tree foliage development was interpreted as a space-filling process for light interception by leaves. Hence, the textural heterogeneity (MIG) of plant communities viewed sideways, or viewed with an overhead angle like in the present study, may in fact decrease if the plant modules are more densely packed per unit of volume. Simply stated, as a community grows denser, MIG may decrease because larger plant modules are occluding smaller ones.

Models of the plant diversity–structural complexity relationship

We simulated gray-tone images to further explore how the size distribution and orientation probability of plant modules relate to the geometric pattern of grassland communities. Our simulations indicated that the relationship between species richness, development time and structural heterogeneity metrics (MIG and anisotropy) could be captured by a dead-leaves model of community assembly. The model simulated the random placement of ellipsoid objects with varying gray tones, sizes and shapes. Our interpretation of this model relies on the assumptions that the anisotropy of a grassland image increases with increasing plant species richness and that the size distribution of plant modules within the image is, for the most part, affected by plant growth. That being said, the similarities between the observed and simulated relationships are remarkable and, thus, beg for further investigation of the model assumptions in natural communities.

How realistic are dead-leaves model simulations of natural vegetation patterns? Although the dead-leaves model-simulated images represent an abstraction of real-world geometric patterns, the model is known to reproduce several statistical properties of natural images (Lee *et al.* 2001). As such, the dead-leaves model may be considered a simple implementation of a couple of key factors affecting the geometry of plant communities, those factors being the size distribution and the orientation pattern of plant modules. The fact that we found

such a close correspondence between observed and simulated images suggested that the geometric structure of grassland communities could be adequately characterized by the size distribution of plant modules, along with any other descriptors that may determine the orientation of plant modules. Other such descriptors likely include plant density, leaf angularity and signs of senescence due to pathogen infections or lack of resources.

We also investigated whether rapidly assessed descriptors of grassland communities were associated with MIG and anisotropy values calculated from gray-tone images. While we did observe a significant relationship between both structural heterogeneity metrics and flowering intensity, this community descriptor explained little of the residual variation. In contrast, mean plant height alone explained up to 38 and 27% of the variation in MIG and anisotropy values, respectively. An initial account of this finding is that taller plant communities displayed more inter-individual variations in height, inducing less heterogeneity and higher anisotropy in the spatial arrangement of biological structures due to a ‘packing density’ effect. This explanation seems well supported by our data, as we found a strong positive correlation ($r = 0.85$) between the mean and standard deviation of inter-individual plant heights within our 234 surveys of grassland communities (78 experimental plots \times 3 growth periods). However, in the experimental design of the Jena Experiment, vegetation height, plant density and flowering intensity were all positively correlated to species richness and may represent confounding effects (e.g. Ebeling *et al.* 2008; Marquard *et al.* 2009).

CONCLUSION

The proposed methodological framework requires only basic knowledge of photographic principles and allows batch processing of a large number of images to calculate structural heterogeneity metrics from existing algorithms. We estimate that, over a single day, one walking photographer can assess the structural heterogeneity of 1500 acres of grasslands at high spatial resolution. Moreover, in the course of our investigation, we noted that MIG values from gray-tone digital images are very strongly, and linearly, correlated to the bit sizes of the low-compression JPEG files. The correlation arises from the fact that spatially heterogeneous digital images are less efficiently compressed than images showing coarser spatial patterns. If the generality of this relationship were confirmed for other cameras and photographic settings, field investigators would have access to a simple and direct measure of structural heterogeneity. While we believe the present study provides compelling evidence that structural heterogeneity is a strong indicator of changes in the growth and species composition of grassland plant communities, future studies should look to refine and test the mechanisms that explain the relationships observed between community-level descriptors and image-derived measures of texture.

FUNDING

German Research Foundation (FOR 456); Natural Sciences and Engineering Research Council of Canada (R.P.).

ACKNOWLEDGEMENTS

We would like to thank the gardeners and numerous student helpers for weeding and mowing of the experimental plots. I.T.R. and F.S.C. were supported by an ERASMUS scholarship. R.P. analyzed the data and wrote the manuscript; other authors provided editorial advice. C.W. and R.P. designed the photographic protocol.

Conflict of interest statement. None declared.

REFERENCES

- Bellis LM, Pidgeon AM, Radeloff VC, *et al.* (2008) Modeling habitat suitability for Greater Rheas based on satellite image texture. *Ecol Appl* **18**:1956–66.
- Carroll SB (2001) Chance and necessity: the evolution of morphological complexity and diversity. *Nature* **409**:1102–9.
- Christensen V (1995) Ecosystem maturity-towards quantification. *Ecol Model* **77**:3–32.
- Cornelissen JHC, Lavorel S, Garnier E, *et al.* (2003) A handbook of protocols for standardised and easy measurement of plant functional traits worldwide. *Aust J Bot* **51**:335–80.
- Crimmins MA, Crimmins TM (2008) Monitoring plant phenology using digital repeat photography. *Environ Manage* **41**:949–58.
- Ebeling A, Klein AM, Schumacher J, *et al.* (2008) How does plant richness affect pollinator richness and temporal stability of flower visits? *Oikos* **117**:1808–15.
- Getzin S, Wiegand K, Schöning I (2011) Assessing biodiversity in forests using very high-resolution images and unmanned aerial vehicles. *Methods Ecol Evol* **3**:397–404.
- Lee AB, Mumford D, Huang J (2001) Occlusion models for natural images: a statistical study of a scale-invariant dead leaves model. *Int J Comput Vis* **41**:35–59.
- Margalef R (1963) On certain unifying principles in ecology. *Am Nat* **97**:357–74.
- Marks CO, Lechowicz MJ (2008) Alternative designs and the evolution of functional diversity. *Am Nat* **167**:55–66.
- Marquard E, Weigelt A, Roscher C, *et al.* (2009) Positive biodiversity-productivity relationship due to increased plant density. *J Ecol* **97**:696–704.
- Mellin C, Parrott L, Andréfouët S, *et al.* (2012) Multi-scale marine biodiversity patterns inferred efficiently from habitat image processing. *Ecol Appl* **22**:792–803.
- Niklas KJ (1994) Morphological evolution through complex domains of fitness. *Proc Natl Acad Sci USA* **91**:6772–9.
- Odum EP (1969) The strategy of ecosystem development. *Science* **164**:262–70.
- Proulx R, Fahrig L (2010) Detecting human-driven deviations from trajectories in landscape composition and configuration. *Landsc Ecol* **25**:1479–87.
- Proulx R, Parrott L (2008) Measures of structural complexity in digital images for monitoring the ecological signature of an old-growth forest ecosystem. *Ecol Indic* **8**:270–84.
- Proulx R, Parrott L (2009) Structural complexity in digital images as an ecological indicator for monitoring forest dynamics across scale, space and time. *Ecol Indic* **9**:1248–56.
- Reu BZ, Proulx R, Bohn K, *et al.* (2011) The role of climate and plant functional trade-offs in shaping global biome and biodiversity patterns. *Global Ecol Biogeogr* **20**:570–81.
- Roscher C, Schumacher J, Baade J, *et al.* (2004) The role of biodiversity for element cycling and trophic interactions: an experimental approach in a grassland community. *Basic Appl Ecol* **5**:107–21.
- St-Louis V, Pidgeon AM, Clayton MK, *et al.* (2009) Satellite image texture and a vegetation index predict avian biodiversity in the Chihuahuan Desert of New Mexico. *Ecography* **32**:468–80.
- Thorp KR, Dierig DA (2011) Color image segmentation approach to monitor flowering in lesquerella. *Ind Crop Prod* **34**:1150–9.
- von Bertalanffy L (1950) The theory of open systems in physics and biology. *Science* **111**:23–9.
- Weller DE (1989) The interspecific size-density relationship among crowded plant stands and its implications for the $-3/2$ power rule of self-thinning. *Am Nat* **133**:20–41.